HHS Public Access

Author manuscript

Free Radic Biol Med. Author manuscript; available in PMC 2021 February 01.

Published in final edited form as:

Free Radic Biol Med. 2020 February 01; 147: 1–7. doi:10.1016/j.freeradbiomed.2019.12.008.

Quantification of reactive oxygen species production by the red fluorescent proteins KillerRed, SuperNova and mCherry.

John O. Onukwufor[a,1], **Adam J. Trewin**[a,1], **Timothy M. Baran**[b], **Anmol Almast**[a], **Thomas H. Foster**[b], **Andrew P. Wojtovich**[a,*]

[a]University of Rochester Medical Center, Department of Anesthesiology and Perioperative Medicine, Rochester NY, 14642 United States.

[b]University of Rochester Medical Center, Department of Imaging Sciences, Rochester 14642, United States.

Abstract

Fluorescent proteins can generate reactive oxygen species (ROS) upon absorption of photons via type I and II photosensitization mechanisms. The red fluorescent proteins KillerRed and SuperNova are phototoxic proteins engineered to generate ROS and are used in a variety of biological applications. However, their relative quantum yields and rates of ROS production are unclear, which has limited the interpretation of their effects when used in biological systems. We cloned and purified KillerRed, SuperNova, and mCherry - a related red fluorescent protein not typically considered a photosensitizer - and measured the superoxide ($O_2^{\bullet-}$) and singlet oxygen ($^1O_2$) quantum yields with irradiation at 561 nm. The formation of the $O_2^{\bullet-}$ -specific product 2-hydroxyethidium (2-OHE^+) was quantified via HPLC separation with fluorescence detection. Relative to a reference photosensitizer, Rose Bengal, the $O_2^{\bullet-}$ quantum yield ($\Phi O_2^{\bullet-}$) of SuperNova was determined to be 1.5×10^{-3}, KillerRed was 0.97×10^{-3}, and mCherry 1.2×10^{-3}. At an excitation fluence of 916.5 J/cm^2 and matched absorption at 561 nm, SuperNova, KillerRed and mCherry made 3.81, 2.38 and 1.65 μM $O_2^{\bullet-}$/min, respectively. Using the probe Singlet Oxygen Sensor Green (SOSG), we ascertained the $^1O_2$ quantum yield (Φ^1O_2) for SuperNova to be 22.0×10^{-3}, KillerRed 7.6×10^{-3}, and mCherry 5.7×10^{-3}. These photosensitization characteristics of SuperNova, KillerRed and mCherry improve our understanding of fluorescent proteins and are pertinent for refining their use as tools to advance our knowledge of redox biology.

GRAPHICAL ABSTRACT

*Corresponding author: Andrew P. Wojtovich Andrew_wojtovich@urmc.rochester.edu Telephone: +1 585 275 4613.
[1]These authors contributed equally

Conflicts of interest: There are no conflicts of interest to declare.

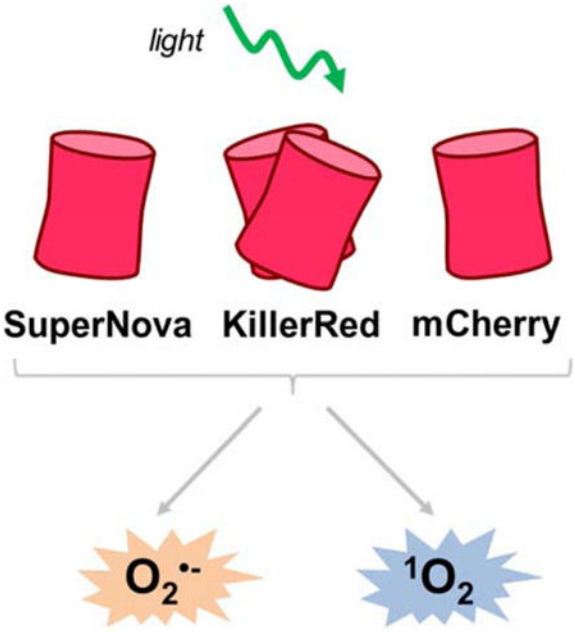

Keywords

redox; optogenetics; superoxide; singlet oxygen; photosensitizer; quantum yield

INTRODUCTION

Fluorescent proteins generate reactive oxygen species (ROS) upon irradiation by type I or type II photosensitization mechanisms [1–4]. The type I mechanism involves electron transfer reactions that ultimately reduce molecular oxygen to form superoxide ($O_2^{\bullet-}$) [3, 5]. Type II photosensitization involves the direct energy transfer from excited triplet state of the photosensitizer to oxygen to generate singlet oxygen ($^1O_2$) [4–7]. Both $O_2^{\bullet-}$ and $^1O_2$ can be formed by fluorescent proteins [4, 5] but the relative yields or fluxes depend on various factors, including the protein structure surrounding the chromophore, the oxygen concentration, temperature, and pH of the environment [3, 5].

A range of phototoxic fluorescent proteins have been developed such as KillerRed, KillerOrange, SuperNova, miniSOG and their derivatives; however their phototoxic properties are not fully characterized [1–3, 8–11]. KillerRed, a dimeric red fluorescent protein, was derived from a random and site-directed mutations of a jellyfish protein, anm2CP [1, 3, 10, 12]. KillerRed has a unique structure with a water channel to the chromophore that is responsible for its phototoxicity [1, 3, 10, 12]. The original KillerRed protein is prone to variable levels of dimerization, which can lead to artifacts and mislocalization of fusion proteins within a biological system [8]. These confounding factors can be mitigated by using the pseudo-monomeric version tandem KillerRed (tdKillerRed), which consists of two repeats of the KillerRed coding sequence, meaning that all copies are expressed as a dimer. SuperNova was derived from KillerRed and retains similar phototoxic properties but exists as a monomer, thereby limiting potential mislocalization events [8].

Both KillerRed and SuperNova are used in a variety of applications ranging from localized ROS production to cell ablation, however the quantities or the species of ROS responsible for the effect are often unclear. KillerRed has been used for chromophore- assisted light inactivation (CALI) in cells and organelles [1, 13–16]. These phototoxic effects have been shown to be sensitive to superoxide dismutase (SOD), catalase, and sodium azide [1, 8], suggesting that KillerRed possesses the capacity to generate both $O_2^{\bullet-}$ (and subsequently hydrogen peroxide) and $^1O_2$ oxidants [1, 2, 8]. Likewise, SuperNova has been shown to oxidize DHE and ADPA probes, implying that it too generates both $O_2^{\bullet-}$ and $^1O_2$ oxidants [8, 17].

Although the phototoxic effects of these fluorescent proteins to cellular functioning have been widely demonstrated, their precise ROS quantum yields, i.e. the ratio of ROS molecules generated per photon absorbed by the fluorophore, and intrinsic rates of ROS production have not previously been reported. Therefore, the aim of this study was to determine the quantum yields and rates of ROS production by phototoxic fluorescent proteins. Using Rose Bengal, a well-characterized chemical photosensitizer molecule with a defined $O_2^{\bullet-}$ quantum yield ($\Phi O_2^{\bullet-}$) of 0.2 and $^1O_2$ quantum yield (Φ^1O_2) of 0.75 as a standard [18], we determined the relative $O_2^{\bullet-}$ and $^1O_2$ quantum yields of tdKillerRed and SuperNova. As a negative control for photosensitization we used mCherry, a red fluorescent protein commonly used as an ‘inert’ fluorophore in many cellular imaging applications [3, 8]. Overall, we report the $O_2^{\bullet-}$ and $^1O_2$ quantum yield of the fluorescent proteins tdKillerRed and SuperNova, as well as mCherry.

MATERIALS AND METHODS

Protein cloning and purification

SuperNova, tdKillerRed, and mCherry were transformed and grown in a culture as previously described [8, 17]. SuperNova/pRSETB was a gift from Dr. Takeharu Nagai (Addgene plasmid # 53234) [8]. mCherry (pmCherry-C1) and tdKillerRed (#FP963, Evrogen) were amplified and ligated into pRSETB using BamHI and EcoRI. Plasmids were then transfected into JM109 (DE3) XJ autolysis cells, and protein expression was induced with isopropyl β-D-1-thiogalactopyranoside (IPTG) resulting in the production of His-tagged SuperNova, tdKillerRed, or mCherry. Cultures were centrifuged at 3200 g for 10 min, washed with PBS and flash frozen. Cell lysate was run through nickel beads, then protein was eluted with 100 μM imidazole in the presence of protease inhibitors (Roche) and desalted using a PD-10 column. Protein concentration was determined by Lowry assay, and absorbance scans were performed on a spectrophotometer (Shimadzu) to identify a region of spectral overlap in absorbance maxima between the proteins and Rose Bengal dye (# 330000, Sigma). The most robust overlap occurred between 550–580 nm (Fig. 1). Based on this, a 561 nm laser was chosen for subsequent experimentation. Proteins and Rose Bengal were diluted to achieve equal molar absorptivity at 561 nm using the Beer-Lambert equation (Table 1).

Irradiation parameters

Irradiation of fluorescent proteins and the photosensitizing dye, Rose Bengal, was performed using a 561 nm class IIIb 50 mW diode laser (#1230935, Coherent® OBIS™, Edmund Optics, NJ, USA). The 0.7 mm diameter beam was focused through a 20x, 0.4 NA microscope objective lens (Swift) into a 200 μm core diameter, 0.22 NA SMA-terminated fiber optic cable (Part # M25L05, ThorLabs, Inc., Newton, NJ) for delivery to the sample. The fiber and objective lens were positioned using a Multimode Fiber Coupler Assembly (Part # F-91-C1-T, Newport Corporation, Irvine, CA). Fiber output was collimated with an aspheric lens (Part # A397TM-B, Thorlabs) to create a 2.5 mm-diameter collimated beam to irradiate each 200 μL sample volume contained within a 1.5 mL, 1 cm polystyrene cuvette (#97000–586, VWR). The irradiance was measured as 25 mW at the front surface of the sample cuvette using thermopile detector (818P-010–12, Newport Corporation, Irvine, CA) for all irradiation. Fluence (light dose, J/cm^2) was modulated by adjusting irradiation time while maintaining a consistent fluence rate (mW/cm^2).

Determination of photobleaching rates

Photobleaching rates of photosensitizers (Rose Bengal, 0.0026 mg/ml; mCherry, 0.22 mg/ml; tdKillerRed, 0.25 mg/ml; SuperNova, 0.76 mg/ml) and the probe DHE alone and in combinations were determined in buffer (D-MRB; 220 mM Manitol, 70 mM Sucrose, 5 mM MOPS, 2 mM EGTA, 0.4% FFBSA, 0.1 mM DTPA, pH 7.3) at 20 °C. The fluorescence signal (Ex 525 nm; Em 550 nm) was acquired using a fluorescence spectrophotometer (Cary Eclipse, Agilent Technologies) during a cumulative time exposure (0–30 min) at 561 nm irradiation for determination of the reduction in fluorescence. To determine the bleaching rates with SOSG, DHE was replaced with SOSG in the buffer, and the change in absorbance was measured between 400 – 800 nm using a spectrophotometer.

Xanthine oxidase superoxide production

Xanthine oxidase (XO) production of $O_2^{\bullet-}$ was determined as the rate of SOD-sensitive cytochrome *c* reduction, as previously described [7, 19]. Briefly, XO (0.25, 0.50, 1.0 and 4.0 mU/mL) was added to a 1 cm cuvette containing cytochrome *c* (40 μM) in PBS containing DTPA (D-PBS: 7.78 mM Na_2HPO_4, 2.20 mM KH_2PO_4, 0.1 mM DTPA, pH 7.3). All reactions were carried out at ambient O_2 and where indicated catalase (4200 U/mL) or SOD (800 U/mL) was present. Baseline measurements were collected for 2 min before 1 mM of xanthine (X) was added to initiate the reaction. Cytochrome *c* reduction was monitored at 550 nm for 10 min, and the rate was calculated using an extinction coefficient of 18.7 mM^{-1} cm^{-1} [20].

Superoxide quantification

The oxidation of dihydroethidium (DHE) yields the $O_2^{\bullet-}$ specific fluorescent product 2-hydroxyethidium ($2\text{-}OHE^+$) along with non-specific fluorescent products including ethidium (E^+), which were separated using HPLC as previously described [7, 17, 21, 22]. Briefly, XO (4 mU/mL) and X (1 mM) were incubated in D-PBS at 20 °C for the indicated time (0 – 60 min). Rose Bengal (0.0026 mg/mL), mCherry (0.22 mg/ml), tdKillerRed (0.25 mg/ml), or SuperNova (0.76 mg/ml) were irradiated at 561 nm for the indicated time (0 – 30 min) in D-

MRB in the presence of DHE (100 μM). For experiments containing photosensitizers, the absorbance was measured (400–800 nm) both pre- and post-irradiation at 561 nm. To these samples, an equal volume of 200 mM $HClO_4$/MeOH was added, centrifuged at 17,000 × *g*, and the supernatant transferred to an equal volume 1 M $K^+PO_4^-$ at pH 2.6.

Samples were separated using a Polar-RP column (Phenomenex, 150 × 2 mm; 4μm) on a Shimadzu HPLC with fluorescence detection (RF-20A). The flow rate was constant (0.1 mL/min) using a gradient of two mobile phases (A: 10% ACN, 0.1 %TFA; B: 60% ACN, 0.1 %TFA). The gradient was the following: 0 min, 40% B; 5 min, 40% B; 25 min, 100% B; 30 min, 100% B; 35 min, 40% B; 40min, 40% B. Standard curves were generated against known concentrations of E^+ and 2-OHE^+, and peaks were quantified using Lab Solutions (Shimadzu) [7, 17].

Singlet oxygen quantification

The $^1O_2$ production of photosensitizers (Rose Bengal, 0.0026 mg/mL; mCherry, 0.22 mg/ml; tdKillerRed, 0.25 mg/ml; SuperNova, 0.76 mg/ml) was measured using SOSG (1 μM, #S36002, Invitrogen) in D-MRB at 20°C [7]. The SOSG signal (Ex 525 nm; Em 550 nm) was acquired using a Cary Eclipse fluorescence spectrophotometer (Agilent Technologies) pre- and post- 561 nm irradiation for determination of the change in SOSG fluorescence intensity [7].

Calculations and statistical analysis

Fluorescent protein $O_2^{\bullet-}$ and $^1O_2$ quantum yields were determined after correcting for the bleaching rates of the photosensitizers, as we have previously demonstrated the importance of photobleaching in explaining time-dependent ROS production by photosensitizers [23]. Measurements of fluorescence and absorbance vs. illumination time were first normalized to the value prior to illumination, and then fit with an equation of the form $B(t) = ae^{-bt}$, where a and b are fit coefficients and t is the illumination duration in seconds. The total number of absorbed photons for a sample can then be expressed as $A = A_0\int_0^{t_d} B(t)dt$, where A_0 is the absorption prior to illumination, t_d is the illumination duration, and $B(t)$ is the bleaching curve described above. Relative to a reference quantum yield (Φ_R), the quantum yield of a sample (Φ_S) can be determined by $\Phi_S = \frac{\text{outs}/A_s}{out_R/A_R} \cdot \Phi_R$,where out is the output of interest and A is the total number of absorbed photons, as described above. Incorporating correction for bleaching of the sample and reference, with knowledge that pre-illumination (A_0) is equal for all samples, the quantum yield can be expressed as:

$$\Phi_S = \frac{out_S}{out_R} \cdot \frac{\int_0^{t_R} B_R(t)dt}{\int_0^{t_S} B_s(t)dt} \cdot \Phi_R$$

where out_S *and* out_R are measured outputs for illumination durations of t_S and t_R for the sample and reference, respectively, and B_s and B_R are the corresponding bleaching curves. All fitting and calculation was performed in MATLAB (The MathWorks, Inc., Natick, MA).

$O_2^{\bullet-}$ production rates of the fluorescent proteins were calculated based upon the standard curve generated using X/XO. Since the apparent number of $O_2^{\bullet-}$molecules required to generate one 2-OHE^+ molecule is dependent on the rate of $O_2^{\bullet-}$, photosensitizer $O_2^{\bullet-}$ production was matched with 4 mU/mL XO superoxide generation. Under these conditions X/XO produced 2.24 μM $O_2^{\bullet-}$/min. X/XO was incubated (0–60 min) of DHE and 2-OHE^+ was measured and plotted against the expected cumulative $O_2^{\bullet-}$ concentration generated during that time, as previously described [7]. At these lower rates the ratio of $O_2^{\bullet-}$ to 2-OHE^+ was linear ($y = 55.62(x) + 326.2$; $R^2 = 0.98$).

Statistical analysis: Data were first tested for normality of variance and were then analyzed by one- or two-way ANOVA with Tukey's post hoc using GraphPad Prism (v7).

RESULTS

Purification and characterization of fluorescent proteins.

Fluorescent proteins subjected to SDS-PAGE migrated at their expected molecular weight (Supplemental Fig. 1). In order to measure protein photosensitization characteristics relative to a reference dye (Rose Bengal), we first sought to determine i) a wavelength that was near the absorption maxima for each chromophore, ii) a concentration of each chromophore in solution that would allow all of the photosensitizers absorb an equal number of photons and iii) is not confounded by absorption of photons by other reagents used for detection of ROS. We determined from absorbance spectra that excitation at 561 nm met each of these criteria (Fig. 1), and photosensitizer concentrations were then optically matched for equal absorbance at 561 nm (Table 1).

Superoxide quantum yield and superoxide generation rate of fluorescent proteins

We measured light-dependent photosensitizer $O_2^{\bullet-}$ generation using HPLC to quantify 2-OHE^+, a $O_2^{\bullet-}$ specific reaction product of DHE [7, 24–26]. Since the known yield of Rose Bengal served as our reference, we confirmed that Rose Bengal produced 2-OHE^+ in a light dose-dependent manner (Fig. 2A) as we have previously demonstrated [7]. Similarly, the fluorescent proteins tdKillerRed, SuperNova and mCherry also produced 2-OHE^+ in a light dose-dependent manner (Fig. 2B), yet the magnitude of 2-OHE^+ for the protein photosensitizers was considerably lower than that of Rose Bengal. For example, after 60 seconds of illumination Rose Bengal generated ~17,000 pmol/mL 2-OHE^+, while after 300 seconds the fluorescent proteins produced ~500 pmol/mL (Fig. 2B).

Next, we sought to determine the $O_2^{\bullet-}$ quantum yield of tdKillerRed, SuperNova and mCherry relative to Rose Bengal, with a known $\Phi O_2^{\bullet-}$ of 0.2 [18]. The determination of quantum yields relies on the equal absorbance of photons, yet photobleaching results in a decrease in photon absorbance over time that occurs at different rates between photosensitizers. Moreover, the bleaching rates of individual fluorescent proteins can be altered depending on the experimental conditions and the presence of small molecules, such as DHE [27]. We therefore measured the rate of photosensitizer bleaching by assessing the change in fluorescence in response to a cumulative light-dose. Surprisingly, we found that DHE promoted the photobleaching of Rose Bengal, mCherry, and SuperNova. We then

corrected for the bleaching rates of the individual fluorophores and the probe, DHE, (Supplemental Fig. S2) in order to calculate the $\Phi O_2^{\bullet-}$ relative to Rose Bengal. We thus determined that SuperNova had a $\Phi O_2^{\bullet-}$ of 1.5×10^{-3}, and tdKillerRed's $\Phi O_2^{\bullet-}$ was 0.97×10^{-3}; mCherry had a comparable $\Phi O_2^{\bullet-}$ (Table 2).

We next sought to calculate the $O_2^{\bullet-}$ production rate of fluorophores. However, the apparent ratio of $O_2^{\bullet-}$ molecules necessary to form one molecule of 2-OHE^+ is highly dependent of the rate of $O_2^{\bullet-}$ generation, possibly due to competition with spontaneous dismutation [7, 26]. Therefore, we generated a standard curve using a concentration of xanthine oxidase that produces $O_2^{\bullet-}$ at a similar rate to that of the photosensitizers. Based on the results of the dose response (Supplementary Fig. S3), we selected 4 mU/mL of xanthine oxidase (Fig. 3A) to match the 2-OHE^+ production rates from our photosensitizers at this concentration and light dose. We determined that 4 mU/mL of xanthine oxidase produces 2.44 μM/min of $O_2^{\bullet-}$, which was SOD-sensitive and catalase-insensitive (Fig. 3A). We incubated the same amount of xanthine oxidase in the presence of DHE, measured the formation 2-OHE^+ over time and expressed it as a function of expected cumulative $O_2^{\bullet-}$ production. Our results show a linear increase of 2-OHE^+ with increasing amounts of $O_2^{\bullet-}$ across the tested range ($R^2 = 0.98$; Fig. 3B). Given that the photosensitizers absorbed an equal amount of light and hence have the same ability to make ROS (Fig. 1, Table 1), we then used this equation to derive the rate of $O_2^{\bullet-}$ production by photosensitizers per unit light dose (Fig. 3C & D) from the data in Fig. 2. Rose Bengal had the highest rates of $O_2^{\bullet-}$ production across light doses (~300 μM $O_2^{\bullet-}$/min at 30.55 J/cm^2) with mCherry producing the least amount $O_2^{\bullet-}$per light dose (~1.65 μM $O_2^{\bullet-}$/min at 916.5 J/cm^2) (Fig. 3C & D). The rate of $O_2^{\bullet-}$ production by Rose Bengal decreased with increasing light dose, which is consistent with the bleaching rate of Rose Bengal (Supplemental Fig. 2). The progressive loss of absorption resulted in a fluence-dependent decrease in the $O_2^{\bullet-}$ production rate. At the light doses tested, each of the fluorescent proteins showed an increasing $O_2^{\bullet-}$ production rate that reached a plateau around 600 J/cm^2 (Fig. 3D). The gradual increase in the measured $O_2^{\bullet-}$ production rate could be due to the modification of local reaction sites, such as amino acids, that can quench $O_2^{\bullet-}$, or a conformational change in the protein resulting in a maximal observed production rate, as has been reported for other fluorescent proteins [28]. As the fluorescent proteins bleach at a slower rate compared to Rose Bengal (Supplemental Fig. 2), we did not observe the same decrease in $O_2^{\bullet-}$ production rate that was detected for Rose Bengal. Additionally, the observed plateau in $O_2^{\bullet-}$ production rate could be the result of increased spontaneous dismutation or the formation of subsequent ROS. Increased $O_2^{\bullet-}$ concentrations can lead to increased dismutation rates, thereby limiting the amount of $O_2^{\bullet-}$ available to react with DHE. The dismutation of $O_2^{\bullet-}$ can form hydrogen peroxide, which via the Fenton reaction generates the hydroxyl radical. Both hydrogen peroxide and the hydroxyl radical can lead to protein modifications that may alter photosensitization rates.

Singlet oxygen quantum yield of fluorescent proteins

Singlet oxygen sensor green (SOSG) specifically detects $^1O_2$ [4, 7, 28, 29] and does not react with other ROS, such as $O_2^{\bullet-}$ or the hydroxyl radical, making it a suitable $^1O_2$ detector under conditions were multiple ROS are being generated [30]. We assessed the $^1O_2$ production of the photosensitizers by measuring the relative change of SOSG fluorescence

and correcting for the bleaching rate of the individual fluorophores (Supplemental Fig. 2) [18]. Rose Bengal had the greatest SOSG fluorescence change with irradiation time (Fig. 4A) relative to those of the fluorescent proteins (Fig. 4B). The Φ^1O_2 of the fluorescent proteins were then calculated relative to the Rose Bengal reference Φ^1O_2 of 0.75 [18]. We determined that SuperNova had the highest Φ^1O_2 at ~22.0×10^{-3}, while mCherry had the lowest Φ^1O_2 of ~5.7×10^{-3} (Table 2, Table 3). This demonstrates that mCherry, tdKillerRed and SuperNova are each capable of generating $^1O_2$ in an irradiation-dose-dependent manner.

DISCUSSION

The main findings from this study are that the red fluorescent proteins tdKillerRed, SuperNova, and mCherry each generate $O_2^{\bullet-}$ and $^1O_2$ via type I and II mechanisms, respectively. We also report for the first time quantitative ROS quantum yields for the fluorescent proteins.

Genetically-encoded photosensitizers are used in a variety of biological applications to generate ROS in a light-dependent manner. They have the advantage of being targeted to precise regions in the cell to provide spatial control over ROS production [2]. However, their precise ROS-producing characteristics have not previously been characterized in detail, particularly in regards to fluorescent protein $\Phi O_2^{\bullet-}$, perhaps as a result of the limited methods to selectively detect $O_2^{\bullet-}$. One study has reported the $\Phi O_2^{\bullet-}$ and Φ^1O_2 of red fluorescent protein, TagRFP [4]. Using a similar SOSG detection approach, the Φ^1O_2 was estimated at 0.004, while the $\Phi O_2^{\bullet-}$ was estimated at <0.0002 using DHE bleaching as a measure of $O_2^{\bullet-}$ [4].

The first developed photosensitizer protein, KillerRed, was initially reported to make $O_2^{\bullet-}$ and $^1O_2$ [1,10]. Subsequently, literature has suggested that the KillerRed photosensitization mechanism selectively produces $O_2^{\bullet-}$ and relies on the water channel to the chromophore for its phototoxicity [10, 31]. Depending on the application, one type of ROS may predominate in contributing to the light-induced effect. For example, $^1O_2$ produced by KillerRed played a role in inactivating a tagged protein in chromophore assisted light inactivation (CALI) experiments [1], while $O_2^{\bullet-}$ generated by KillerRed was shown to mediate phototoxicity at the cellular level [32]. While our results demonstrate that both $^1O_2$ and $O_2^{\bullet-}$ are capable of being produced, researchers should consider which species is relevant to their particular biological application using ROS-selective scavengers or reaction products.

SuperNova was derived from KillerRed, and it would be reasonable to assume that the photosensitization mechanisms would be similar. Accordingly, SuperNova has been thought to produce $O_2^{\bullet-}$ and $^1O_2$, as measured by 2-OHE$^+$ formation [17] and ADPA photobleaching [8], respectively. In the present study, SuperNova's comparatively larger ROS quantum yield than tdKillerRed (Table 3) is consistent with previous reports of greater phototoxicity [8]. Specifically, at 916.5 J/cm^2 of fluence, we show that the SuperNova $O_2^{\bullet-}$production rate is ~1.55 fold higher than tdKillerRed (Table 3). However, the $O_2^{\bullet-}$ production rate was not consistent across fluences tested, and plateaued at the highest light dose tested. While the quantum yields provide a direct comparison of the phototoxic mechanisms of the red fluorescent proteins tested, caution is warranted when extrapolating these findings *in vivo*.

The O_2 and pH gradients or endogenous chromophores present in the cellular milieu can affect the ROS generation by photosensitizers. For example, a high O_2 tension could favor $^1O_2$ production, while hypoxic conditions could favor $O_2^{\bullet-}$ production [33].

Unlike KillerRed and SuperNova that were derived from the jellyfish protein anm2CP, mCherry was derived from the sea anemone protein DsRed. Owing to the structural differences that exist due to their independent lineage, mCherry lacks a water channel, suggesting that it would not be as phototoxic as KillerRed. Indeed, it is widely used in biological applications under the assumption that it is photochemically inert. However, some previous reports have also shown that mCherry can be phototoxic [34] and that it produces $O_2^{\bullet-}$ [8, 35] and $^1O_2$ [8] upon irradiation. Our present findings are in agreement with this and indicate that mCherry displays $\Phi O_2^{\bullet-}$ and Φ^1O_2 that are comparable to the 'professional' photosensitizer proteins. The potential implication of this is that the use of mCherry as an imaging tool, such as for live microscopy experiments, could inadvertently introduce non-trivial confounding variables resulting from redox signaling events and/or oxidative distress [36]. Similar concerns were recently described for the expression of green fluorescent protein (GFP) [37]. Although independent of irradiation, the overexpression of GFP activated redox sensitive signaling pathways [37]. Our findings suggest that long-term imaging with mCherry could alter the redox environment. Care should therefore be taken to express mCherry at the lowest useable level, to minimize the intensity and duration of irradiation during these experiments, and validate findings with alternative methodologies.

The genetically-encoded photosensitizers display $\Phi O_2^{\bullet-}$ and Φ^1O_2 that were measured as being orders of magnitude lower than the chemical photosensitizer Rose Bengal. Nevertheless, our current Φ^1O_2 findings are generally in agreement with other fluorescent proteins that have been reported to range from Φ^1O_2 0.004 to 0.030 [3]. Recently, optimized variants have reportedly reached Φ_1O_2 ~0.6 [38]. New approaches are aimed at combining the large quantum yields of chemical photosensitizers with the advantages of genetically-encoded photosensitizers [39]. It should be noted that despite being an *in vitro* experiment essentially consisting of only the photosensitizer and probe, many factors can affect the stoichiometry of the reaction between $O_2^{\bullet-}$ and DHE to result in 2-OHE^+ such as the protein concentration, susceptible amino acids exposed to the solvent, the presence of other targets in the milieu, and the rate of oxidant production. In relation to the latter, we attempted to account for this by matching the rate of $O_2^{\bullet-}$ generation relative to that of the known rates in the X/XO system. A likely explanation for the lower rates of oxidant formation is that once formed by the excited chromophore, the $O_2^{\bullet-}$anion or $^1O_2$ must escape the protein barrel structure in order to be released to the surrounding environment and react with the ROS probe [10]. The protein barrel likely shields the release of ROS, potentially explaining the lower observed $\Phi O_2^{\bullet-}$of the protein photosensitizers compared to Rose Bengal which can directly release oxidants to the surrounding aqueous environment. It is likely that the protein concentration, as well as the number of oxidant-susceptible amino acids exposed to the solvent, can influence the amount of ROS available to react with other biological targets. Yet, despite their lower quantum yields, the ability for the photosensitizer proteins to generate a biologically relevant effect is well established. For example, when KillerRed is expressed at multi-copy levels, protein inactivation and cell death occurs with photoactivation [1, 2, 8, 17]. Yet when SuperNova is expressed as single-copy, lower levels

of oxidant generation can lead to induction of redox sensitive signaling pathways that promote adaptive responses [17]. Overall, factors that define a biologically relevant amount of ROS are highly context dependent since the effects of ROS are highly spatially and temporally dependent [3, 40, 41].

Conclusion

Overall, we demonstrate that the red fluorescent proteins tdKillerRed, SuperNova and mCherry are able to photosensitize $O_2^{\bullet-}$ and $^1O_2$. Our studies provide $\Phi O_2^{\bullet-}$, Φ^1O_2 and rates of $O_2^{\bullet-}$ production across light doses. Our findings will help elucidate mechanisms mediated by phototoxic proteins and aid in the development of efficient or selective ROS production by genetically-encoded photosensitizers [38, 42].

Supplementary Material

Refer to Web version on PubMed Central for supplementary material.

ACKNOWLEDGEMENTS

We thank the members of the mitochondrial research group at the University of Rochester Medical Center for their valuable suggestions and contributions. AJT current address: Institute for Physical Activity and Nutrition (IPAN), School of Exercise and Nutrition Sciences, Deakin University, Burwood, VIC, Australia.

Disclosure of funding: This work was funded by a grant from the National Institutes of Health to APW (R01 NS092558).

ABBREVIATIONS:

2-OHE$^+$	2-hydroxyethidium
CALI	Chromophore assisted light inactivation
DHE$^+$	Dihydroethidium
E$^+$	Ethidium
$O_2^{\bullet-}$	Superoxide
$^1O_2$	Singlet oxygen
Φ	Quantum yield
$\Phi O_2^{\bullet-}$	Superoxide quantum yield
Φ^1O_2	Singlet oxygen quantum yield
ROS	Reactive oxygen species
SOSG	Singlet oxygen sensor green
SOD	Superoxide dismutase
X	Xanthine

XO	Xanthine oxidase

REFERENCES

[1]. Bulina ME, Chudakov DM, Britanova OV, Yanushevich YG, Staroverov DB, Chepurnykh TV, Merzlyak EM, Shkrob MA, Lukyanov S, Lukyanov KA, A genetically encoded photosensitizer, Nature biotechnology 24(1) (2006) 95–9.

[2]. Wojtovich AP, Foster TH, Optogenetic control of ROS production, Redox biology 2 (2014) 368–76. [PubMed: 24563855]

[3]. Trewin AJ, Berry BJ, Wei AY, Bahr LL, Foster TH, Wojtovich AP, Light-induced oxidant production by fluorescent proteins, Free radical biology & medicine 128 (2018) 157–164. [PubMed: 29425690]

[4]. Ragas X, Cooper LP, White JH, Nonell S, Flors C, Quantification of photosensitized singlet oxygen production by a fluorescent protein, Chemphyschem : a European journal of chemical physics and physical chemistry 12(1) (2011) 161–5. [PubMed: 21226197]

[5]. Krasnovsky AA Jr., Primary mechanisms of photoactivation of molecular oxygen. History of development and the modern status of research, Biochemistry. Biokhimiia 72(10) (2007) 1065–80. [PubMed: 18021065]

[6]. Souslova EA, Mironova KE, Deyev SM, Applications of genetically encoded photosensitizer miniSOG: from correlative light electron microscopy to immunophotosensitizing, Journal of biophotonics 10(3) (2017) 338–352. [PubMed: 27435584]

[7]. Barnett ME, Baran TM, Foster TH, Wojtovich AP, Quantification of light-induced miniSOG superoxide production using the selective marker, 2-hydroxyethidium, Free radical biology & medicine 116 (2018) 134–140. [PubMed: 29353158]

[8]. Takemoto K, Matsuda T, Sakai N, Fu D, Noda M, Uchiyama S, Kotera I, Arai Y, Horiuchi M, Fukui K, Ayabe T, Inagaki F, Suzuki H, Nagai T, SuperNova, a monomeric photosensitizing fluorescent protein for chromophore-assisted light inactivation, Scientific reports 3 (2013) 2629. [PubMed: 24043132]

[9]. Shu X, Shaner NC, Yarbrough CA, Tsien RY, Remington SJ, Novel chromophores and buried charges control color in mFruits, Biochemistry 45(32) (2006) 9639–47. [PubMed: 16893165]

[10]. Carpentier P, Violot S, Blanchoin L, Bourgeois D, Structural basis for the phototoxicity of the fluorescent protein KillerRed, FEBS letters 583(17) (2009) 2839–42. [PubMed: 19646983]

[11]. Westberg M, Holmegaard L, Pimenta FM, Etzerodt M, Ogilby PR, Rational design of an efficient, genetically encodable, protein-encased singlet oxygen photosensitizer, Journal of the American Chemical Society 137(4) (2015) 1632–42. [PubMed: 25575190]

[12]. Bulina ME, Lukyanov KA, Britanova OV, Onichtchouk D, Lukyanov S, Chudakov DM, Chromophore-assisted light inactivation (CALI) using the phototoxic fluorescent protein KillerRed, Nature protocols 1(2) (2006) 947–53. [PubMed: 17406328]

[13]. Shibuya T, Tsujimoto Y, Deleterious effects of mitochondrial ROS generated by KillerRed photodynamic action in human cell lines and C. elegans, Journal of photochemistry and photobiology. B, Biology 117 (2012) 1–12. [PubMed: 23000754]

[14]. Wang B, Van Veldhoven PP, Brees C, Rubio N, Nordgren M, Apanasets O, Kunze M, Baes M, Agostinis P, Fransen M, Mitochondria are targets for peroxisome-derived oxidative stress in cultured mammalian cells, Free radical biology & medicine 65 (2013) 882–894. [PubMed: 23988789]

[15]. Shao LW, Niu R, Liu Y, Neuropeptide signals cell non-autonomous mitochondrial unfolded protein response, Cell research 26(11) (2016) 1182–1196. [PubMed: 27767096]

[16]. Liao ZX, Li YC, Lu HM, Sung HW, A genetically-encoded KillerRed protein as an intrinsically generated photosensitizer for photodynamic therapy, Biomaterials 35(1) (2014) 500–8. [PubMed: 24112805]

[17]. Trewin AJ, Bahr LL, Almast A, Berry BJ, Wei AY, Foster TH, Wojtovich AP, Mitochondrial Reactive Oxygen Species Generated at the Complex-II Matrix or Intermembrane Space Microdomain Have Distinct Effects on Redox Signaling and Stress Sensitivity in Caenorhabditis elegans, Antioxid Redox Signal (2019).

[18]. Lee PC, Rodgers MA, Laser flash photokinetic studies of rose bengal sensitized photodynamic interactions of nucleotides and DNA, Photochemistry and photobiology 45(1) (1987) 79–86. [PubMed: 3031708]

[19]. Kelley EE, Khoo NK, Hundley NJ, Malik UZ, Freeman BA, Tarpey MM, Hydrogen peroxide is the major oxidant product of xanthine oxidase, Free radical biology & medicine 48(4) (2010) 493–8. [PubMed: 19941951]

[20]. Margoliash E, Frohwirt N, Spectrum of horse-heart cytochrome c, Biochem J 71(3) (1959) 570–2. [PubMed: 13638266]

[21]. Zielonka J, Vasquez-Vivar J, Kalyanaraman B, Detection of 2-hydroxyethidium in cellular systems: a unique marker product of superoxide and hydroethidine, Nature protocols 3(1) (2008) 8–21. [PubMed: 18193017]

[22]. Zhao H, Joseph J, Fales HM, Sokoloski EA, Levine RL, Vasquez-Vivar J, Kalyanaraman B, Detection and characterization of the product of hydroethidine and intracellular superoxide by HPLC and limitations of fluorescence, Proceedings of the National Academy of Sciences of the United States of America 102(16) (2005) 5727–32. [PubMed: 15824309]

[23]. Mitra S, Foster TH, Photophysical parameters, photosensitizer retention and tissue optical properties completely account for the higher photodynamic efficacy of meso-tetra-hydroxyphenyl- chlorin vs Photofrin, Photochemistry and photobiology 81(4) (2005) 849–59. [PubMed: 15807635]

[24]. Kalyanaraman B, Hardy M, Podsiadly R, Cheng G, Zielonka J, Recent developments in detection of superoxide radical anion and hydrogen peroxide: Opportunities, challenges, and implications in redox signaling, Archives of biochemistry and biophysics 617 (2017) 38–47. [PubMed: 27590268]

[25]. Zielonka J, Hardy M, Kalyanaraman B, HPLC study of oxidation products of hydroethidine in chemical and biological systems: ramifications in superoxide measurements, Free radical biology & medicine 46(3) (2009) 329–38. [PubMed: 19026738]

[26]. Michalski R, Michalowski B, Sikora A, Zielonka J, Kalyanaraman B, On the use of fluorescence lifetime imaging and dihydroethidium to detect superoxide in intact animals and ex vivo tissues: a reassessment, Free radical biology & medicine 67 (2014) 278–84. [PubMed: 24200598]

[27]. Zheng Q, Jockusch S, Zhou Z, Blanchard SC, The contribution of reactive oxygen species to the photobleaching of organic fluorophores, Photochemistry and photobiology 90(2) (2014) 448–454. [PubMed: 24188468]

[28]. Ruiz-Gonzalez R, Cortajarena AL, Mejias SH, Agut M, Nonell S, Flors C, Singlet oxygen generation by the genetically encoded tag miniSOG, Journal of the American Chemical Society 135(26) (2013) 9564–7. [PubMed: 23781844]

[29]. Gollmer A, Arnbjerg J, Blaikie FH, Pedersen BW, Breitenbach T, Daasbjerg K, Glasius M, Ogilby PR, Singlet Oxygen Sensor Green(R): photochemical behavior in solution and in a mammalian cell, Photochemistry and photobiology 87(3) (2011) 671–9. [PubMed: 21272007]

[30]. Kim S, Fujitsuka M, Majima T, Photochemistry of singlet oxygen sensor green, The journal of physical chemistry. B 117(45) (2013) 13985–92.

[31]. Pletnev S, Gurskaya NG, Pletneva NV, Lukyanov KA, Chudakov DM, Martynov VI, Popov VO, Kovalchuk MV, Wlodawer A, Dauter Z, Pletnev V, Structural basis for phototoxicity of the genetically encoded photosensitizer KillerRed, J Biol Chem 284(46) (2009) 32028–39. [PubMed: 19737938]

[32]. Serebrovskaya EO, Edelweiss EF, Stremovskiy OA, Lukyanov KA, Chudakov DM, Deyev SM, Targeting cancer cells by using an antireceptor antibody-photosensitizer fusion protein, Proceedings of the National Academy of Sciences of the United States of America 106(23) (2009) 9221–5. [PubMed: 19458251]

[33]. Gilson RC, Black KCL, Lane DD, Achilefu S, Hybrid TiO2 -Ruthenium Nano-photosensitizer Synergistically Produces Reactive Oxygen Species in both Hypoxic and Normoxic Conditions, Angew Chem Int Ed Engl 56(36) (2017) 10717–10720.

[34]. Strack RL, Strongin DE, Bhattacharyya D, Tao W, Berman A, Broxmeyer HE, Keenan RJ, Glick BS, A noncytotoxic DsRed variant for whole-cell labeling, Nature methods 5(11) (2008) 955–7. [PubMed: 18953349]

[35]. Hoffmann S, Orlando M, Andrzejak E, Bruns C, Trimbuch T, Rosenmund C, Garner CC, Ackermann F, Light-Activated ROS Production Induces Synaptic Autophagy, The Journal of neuroscience : the official journal of the Society for Neuroscience 39(12) (2019) 2163–2183.

[36]. Icha J, Weber M, Waters JC, Norden C, Phototoxicity in live fluorescence microscopy, and how to avoid it, Bioessays 39(8) (2017).

[37]. Ganini D, Leinisch F, Kumar A, Jiang J, Tokar EJ, Malone CC, Petrovich RM, Mason RP, Fluorescent proteins such as eGFP lead to catalytic oxidative stress in cells, Redox biology 12 (2017) 462–468. [PubMed: 28334681]

[38]. Westberg M, Bregnhoj M, Etzerodt M, Ogilby PR, No Photon Wasted: An Efficient and Selective Singlet Oxygen Photosensitizing Protein, The journal of physical chemistry. B 121(40) (2017) 9366–9371. [PubMed: 28892628]

[39]. He J, Wang Y, Missinato MA, Onuoha E, Perkins LA, Watkins SC, St Croix CM, Tsang M, Bruchez MP, A genetically targetable near-infrared photosensitizer, Nature methods 13(3) (2016) 263–8. [PubMed: 26808669]

[40]. Jones DP, Sies H, The Redox Code, Antioxid Redox Signal 23(9) (2015) 734–46. [PubMed: 25891126]

[41]. Wojtovich AP, Berry BJ, Galkin A, Redox Signaling Through Compartmentalization of Reactive Oxygen Species: Implications for Health and Disease, Antioxid Redox Signal 31(9) (2019) 591–593. [PubMed: 31084372]

[42]. Westberg M, Etzerodt M, Ogilby PR, Rational design of genetically encoded singlet oxygen photosensitizing proteins, Curr Opin Struct Biol 57 (2019) 56–62. [PubMed: 30875586]

HIGHLIGHTS

- We report $O_2^{\bullet-}$ and $^1O_2$ quantum yields for KillerRed, SuperNova and mCherry.
- $O_2^{\bullet-}$ generation was measured using HPLC separation of 2-OHE^+ and $^1O_2$ with SOSG.
- Supernova's $O_2^{\bullet-}$ and $^1O_2$ yields are larger than those of KillerRed and mCherry.
- $O_2^{\bullet-}$ quantum yield of mCherry is comparable to those of KillerRed and SuperNova.

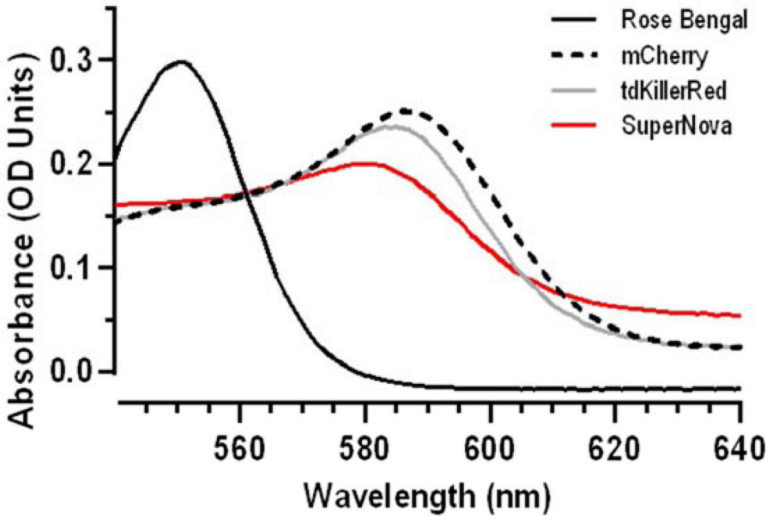

Fig. 1. Equal photosensitizer absorbance at 561 nm.

(a) Absorbance spectrum of the photosensitizers Rose Bengal dye (0.0026 mg/mL), mCherry (0.22 mg/mL), tdKillerRed (0.25 mg/mL), and SuperNova (0.76 mg/mL). See Table 1 for quantification.

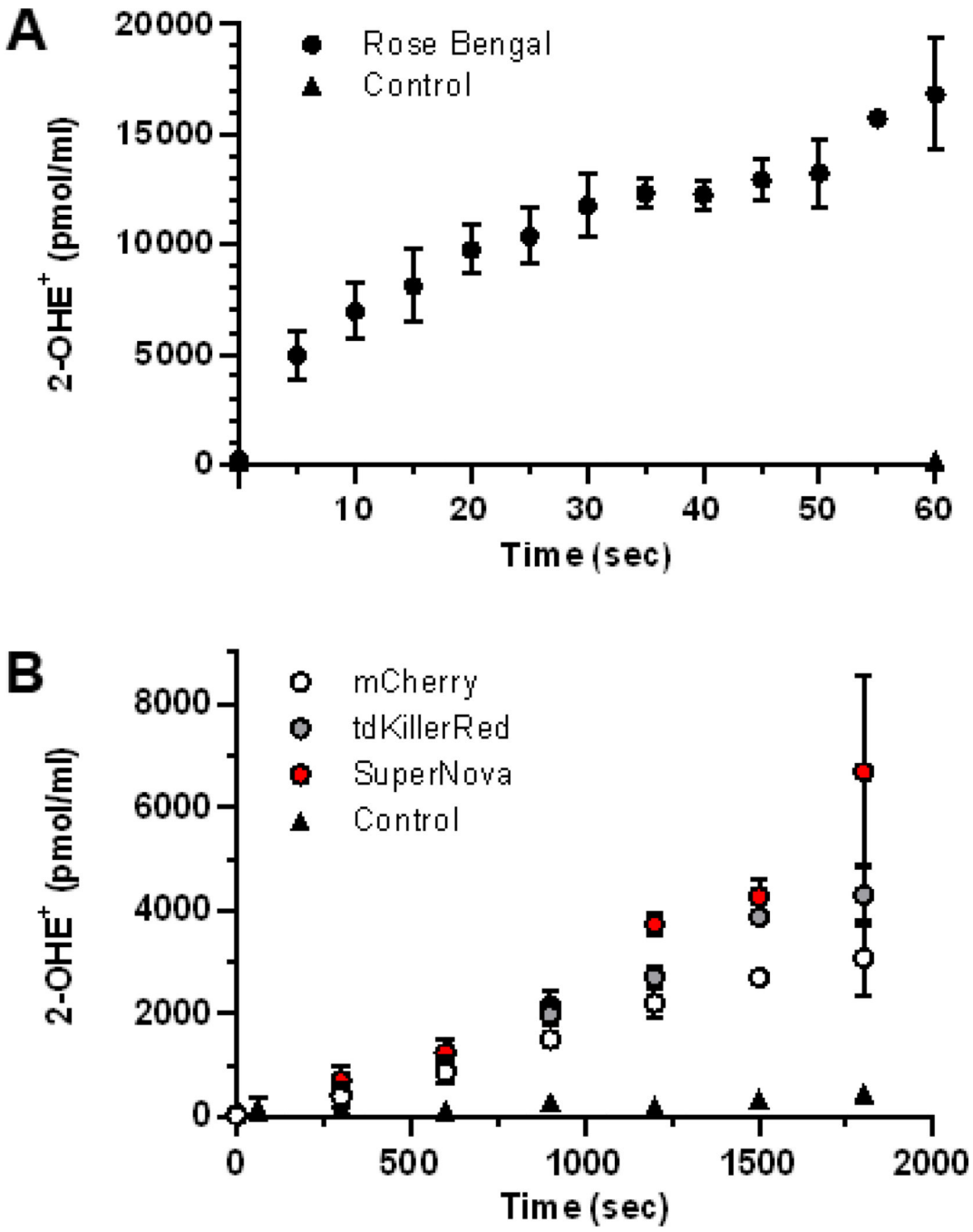

Fig. 2. Light-dependent superoxide generation by photosensitizers.

(a) Rose Bengal, (b) tdKillerRed, Supernova, mCherry and control (no photosensitizer) were irradiated with equal molar absorptivity at 561 nm in the presence of DHE (100 μM) for quantification of 2-OHE$^+$. Values are mean ± SD for n = 3 independent experiments.

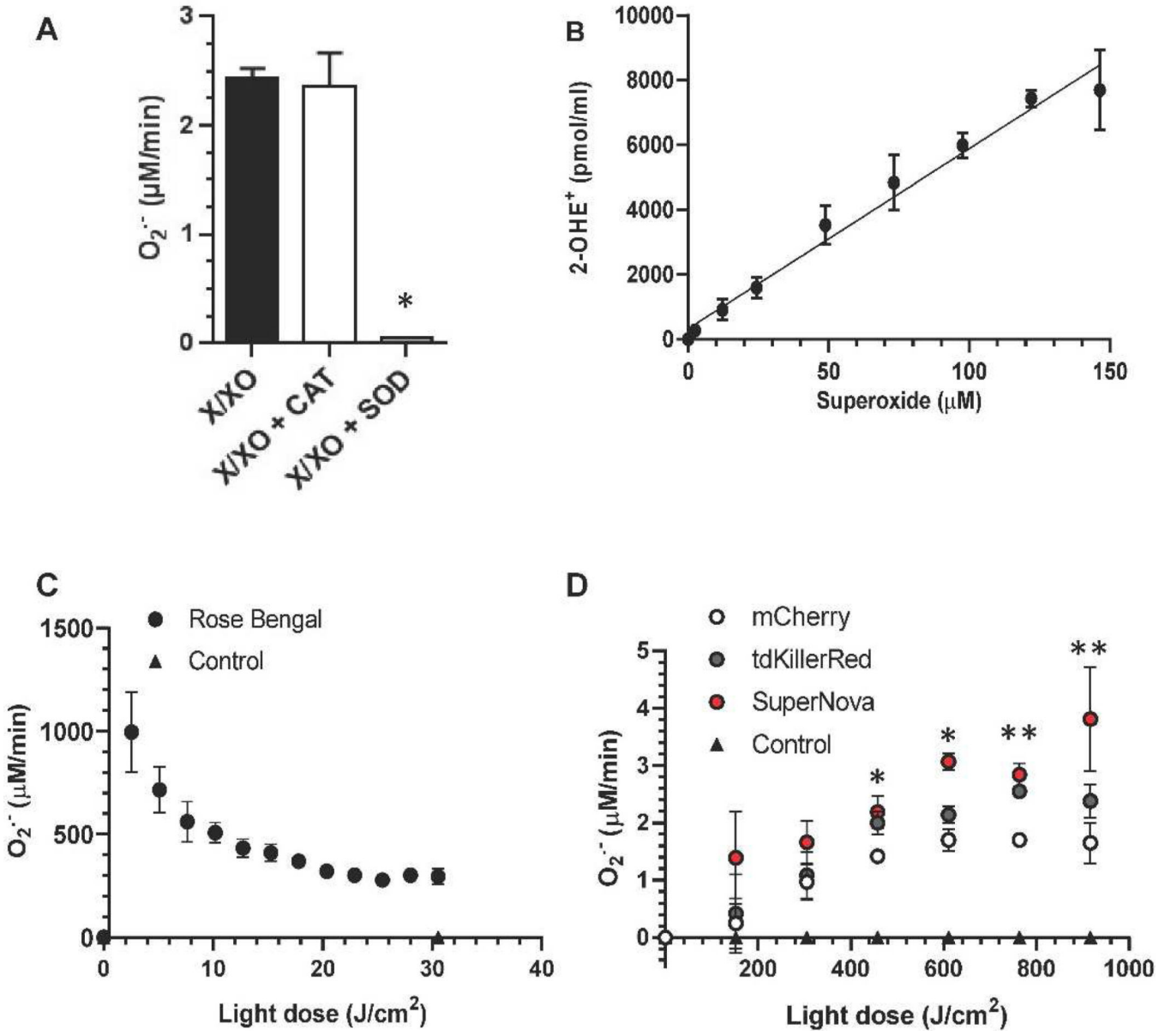

Fig. 3. Determination of superoxide production per light dose.

(a) xanthine/xanthine oxidase (X/XO) $O_2^{\bullet-}$ production was assessed using cytochrome c reduction assay. Xanthine oxidase (XO, 4 mU/mL) and xanthine (X, 1 mM) were incubated with catalase (CAT) superoxide dismutase (SOD) where indicated. * $p < 0.05$ X/XO+SOD vs X/XO and vs X/XO+CAT, one-way ANOVA, Tukey post hoc. (b) Time course (0–60 min) of X/XO $O_2^{\bullet-}$ generation was measured using HPLC separation of 2-OHE$^+$ and then plotted against the expected $O_2^{\bullet-}$ production. (c) Rose Bengal $O_2^{\bullet-}$ production rate per light dose. (d) Fluorescent protein (mCherry, tdKillerRed and SuperNova) $O_2^{\bullet-}$ production per light dose. Data from (c) and (d) are derived from data presented in Fig. 2. *$p < 0.05$ SuperNova vs mCherry, ** $p < 0.05$ SuperNova and tdKillerRed vs mCherry, two-way ANOVA, Bonferroni post hoc. Values are mean ± SD for n = 3 independent experiments.

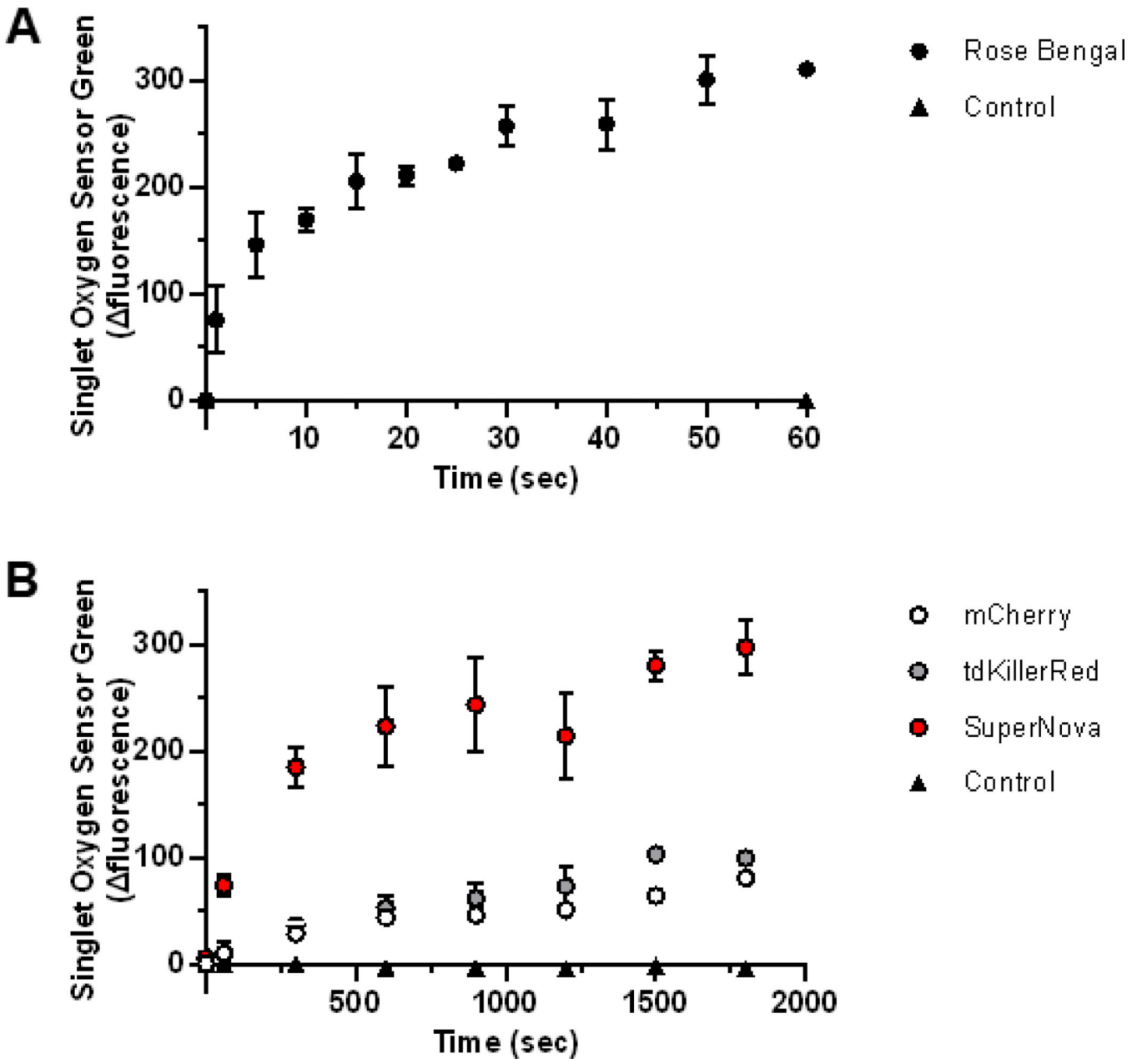

Fig. 4. Singlet oxygen generation by photosensitizers in response to 561 nm irraditation.

(a) Rose Bengal, (b) tdKillerRed, Supernova, mCherry and control (no photosensitizer) were irradiated with equal molar absorptivity at 561 nm in the presence of 0.1 μM SOSG. The initial fluorescence reading (Ex 525 nm; Em 550 nm) was subtracted from the post-illumination reading and presented as the relative fluorescence change. Values are mean ± SD for n = 3 independent experiments.

TABLE 1:

Photosensitizer absorbance at 561 nm.

Photosensitizer	Absorbance (561 nm)
Rose Bengal	0.172±0.008
mCherry	0.170±0.003
tdKillerRed	0.169±0.009
SuperNova	0.172±0.007

Absorbance at 561 nm after concentration adjustment of Rose Bengal dye (0.0026 mg/mL), mCherry (0.22 mg/mL), tdKillerRed (0.25 mg/mL), and SuperNova (0.76 mg/mL). Values are mean ± SD for n = 3 independent experiments; $p > 0.96$ by one-way ANOVA.

TABLE 2:

Superoxide and singlet oxygen quantum yield of mCherry, tdKillerRed, and SuperNova.

Fluorescent protein	$O_2^{\bullet-}$ Quantum yield ($\Phi O_2^{\bullet-}$)	$^1O_2$ Quantum yield (Φ^1O_2)
mCherry	$1.20\pm0.044 \times 10^{-3}$	$5.7\pm0.27 \times 10^{-3}$
tdKillerRed	$0.97\pm0.042 \times 10^{-3}$	$7.6\pm0.26 \times 10^{-3}$
SuperNova	$1.50\pm0.016 \times 10^{-3}$	$22.0\pm1.80 \times 10^{-3}$

Data are mean ± SD for n=3 independent experiments

TABLE 3:

Superoxide and singlet oxygen quantum yield of fluorescent proteins relative to tdKillerRed.

Fluorescent protein	Relative $O_2^{\bullet-}$ yield	Relative $^1O_2$ yield
mCherry	1.24	0.75
tdKillerRed	1.00	1.00
SuperNova	1.55	2.89